Measurement of DC Busbar Currents in Aluminium Smelters

Vinko Potocnik[1], Alexander Arkhipov[2], Nadia Ahli[3] and Abdalla Alzarooni[4]
1. Consultant
2. Manager – Modelling Technology Development and Transfer
3. Manager - Technology Transfer Contracts
4. Vice President Technology Development and Transfer
Emirates Global Aluminium, Dubai, United Arab Emirates
Corresponding author: vinko.potocnik@sympatico.ca

Abstract

Busbar current distribution is an important aluminium electrolysis cell design and operation parameter, which determines the electrical and magnetic equilibrium of the cell. Several methods of measurement of electrical currents in busbars are used in aluminium smelters: voltage probes or forks based on Ohm's law, Rogowski coil clamp-on loops based on electromagnetic induction, magnetic sensors based on Hall Effect and fibre optics current sensors based on Faraday Effect. Some of these devices are fixed on or around the busbars, some are portable. Access to busbars and maximum ambient temperature may be an issue for some devices. The choice of equipment depends on purpose of measurements, accuracy required and cost. In this paper we present and compare the measurement methods and principles, used in aluminium smelters for busbar current measurements, with special emphasis on the latest technology – flexible optical fibre current meter from Smart Digital Optics (SDO). In Emirates Global Aluminium several of these methods are used.

Keywords: Aluminum smelter DC current measurement, millivolt fork, clamp-on current meter, Hall Effect sensors, fibre optics current sensors.

1. Introduction

Electrical current distribution in the busbars and inside the pot is an important parameter of pot design and operation. It determines the magnetic field and current distribution in the liquid aluminium metal pad, which create the electromagnetic forces in the metal pad, responsible for cell magnetohydrodynamic (MHD) characteristics: metal and bath circulation, bath-metal interface deformation and cell instabilities. Current distribution in the busbars between two adjacent pots is determined by busbar design, which is chosen to generate a balanced magnetic field and approximately equal collector bar currents in order to provide MHD equilibrium in the liquid metal of the pot. Current distribution in the cathode collector bars is determined by the busbar and cathode design; it does not change with time, unless the cathode blocks have specific problems, such as cracking or collector bars are attacked by liquid aluminium.

Current distribution in the anode rods mostly depends on the resistance of each individual anode between the anode beam and the liquid metal pad. The largest part of this resistance comes from the thickness of the bath layer below each anode, but also from the bubble coverage of each anode bottom which is a function of local alumina concentration. The resistance on the path through each anode also depends on anode bottom condition (spikes) and on the contact resistance between the anode stubs and anode carbon block. The current of an anode varies over the lifetime of the anode; it is zero or very small for the first few hours after the anode setting and then gradually increases to reach the average value in typically 24 to 48 h. After that it stays more or less constant and is controlled to be within the specified upper and lower limit. The anodes are moved up if the current is above the upper limit and down if the current is below the lower limit; this operation is done with the help of the Pot Tending Machine (PTM) as the pots

usually do not have individual anode drives. Therefore, such adjustments have to be limited in number as the PTM and pot operators have limited availability. However, the automatic control of anode currents on experimental pots with individual anode drives has been reported [1], but it was found out that the number of anode adjustments per day has to be limited in spite of the capability to move the anodes up and down automatically. The reason is that the anodes have a self-adjusting capability for current over time, because anode consumption is proportional to the current density on the bottom face of the anode; if an anode carries more or less than average current, the anode consumption will be faster or slower than the average, which adjusts the local ACD and that the currents tend to equalize.

At pot design stage, busbar and collector bar current distributions are determined with mathematical models, which have to be validated with measurements. Any changes of current distribution in cathode collector bars or anode rods due to pot operation can be determined by measurements only. The measurements of current distribution in the busbars can be periodic or continuous. The measurements of collector bar current distribution are most often periodic and are made for mathematical model validation [2] or for detecting specific condition of the cathode blocks, such as collector bar attack by liquid aluminium [3]. The measurement of anode current distribution is most of the time periodic for the control of anode currents [4]. Continuous measurements of anode currents have been made for automatic anode current control [1] or for research to determine how the anode currents change with specific events such as approaching or real anode effects, local alumina concentration, presence of anode spikes, perfluorocarbon (PFC) emissions, etc. [5 - 8]

In this paper we present the principles of measurement of DC currents and discuss applications of each principle to busbar, cathode collector bar or anode rod current measurements.

2. Principles of DC Current Measurement

Four principles of DC current measurement will be discussed:

1) Measurement of voltage drop between two points on the conductor,
2) Rogowski coil,
3) Hall Effect sensors,
4) Fibre optics current sensors, based on Faraday Effect.

2.1. Measurement of Voltage Drop between Two Points on the Conductor

The simplest and most commonly used method is to measure the voltage drop between two points on a conductor at a fixed distance apart. Two voltage probes, either attached to the busbar (Figure 3.2 and 3.4) or fixed on a portable fork (Figure 3.1) or semi-permanent fork (Figure 3.3 left) are used. Voltage drop is measured by a voltmeter or data logger. In modern portable forks, the voltmeter is attached to the holder [4]. Busbar current is determined from Ohm's Law, Equation (2.1):

$$\Delta V = RI \rightarrow I = \frac{\Delta V}{R} = \frac{\Delta VA}{\rho(T)L} \tag{2.1}$$

where:
- I Measured potline current, kA
- ΔV Measured voltage drop between the two voltage probes, mV
- R Electrical resistance of the conductor between the two probes, Ω
- A Conductor cross-section, m^2
- L Distance between the two probes, m
- $\rho(T_i)$ Electrical resistivity of the conductor, a function of temperature, μΩm
- T Temperature of the conductor between the two voltage probes.

Busbar temperature is measured between the two voltage probes with a surface thermocouple or with a thermocouple fixed to the busbar if voltage probes are attached to the busbar permanently. Optical pyrometer (infrared gun) cannot be used for temperature measurements of aluminium busbars, because the emission coefficient of aluminium busbars may vary in a wide range, depending on busbar surface condition and temperature.

2.2. Rogowski Coil and Clamp-On Current Meters

Rogowski coil is a toroidal coil placed around the conductor. If the current in the conductor varies with time, there is a voltage induced in the coil, given in Equation (2.2):

$$V(t) = -\mu_0 NA\frac{dI}{dt} \rightarrow I = -\frac{1}{\mu_0 NA}\int V(t)dt \qquad (2.2)$$

where: V Induced voltage, V
μ_0 Permeability of vacuum, Vs/Am,
N Number of turns/unit length, m^{-1}
A Area of a turn, m^2
I Current, A
T Time, s
dI/dt Rate of change of the current enclosed by the coil, A/s

For DC current measurements, the variation of current is produced by closing the loop with no conductor inside (Figure 2.1, right) and then closing it around the conductor (Figure 2.1, left). The integration of the impulse gives the current. Figures 2.2 and 2.3 show commercial probes. The accuracy of probes is ± 2.5 %.

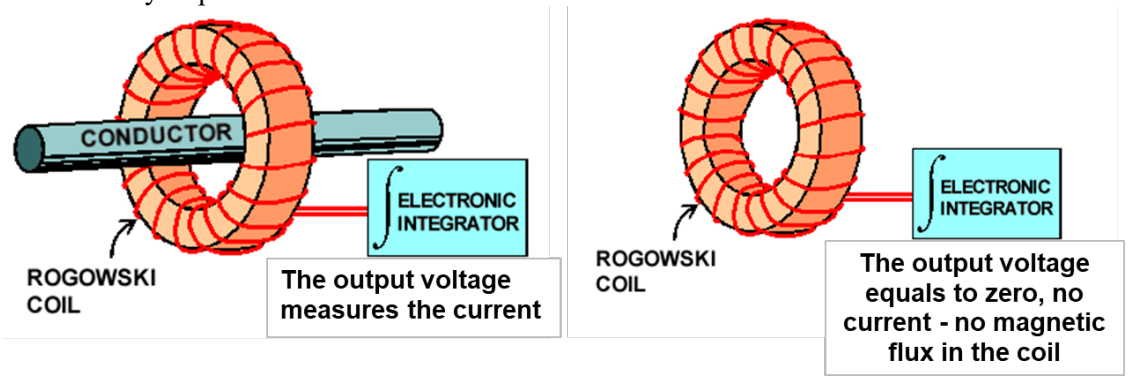

Figure 2.1. Principle of the Rogowski coil for DC current measurement.

Figure 2.2. DynAmp clamp-on portable (COP) current meter.

Closed, opens by rotation Closed Opens by sliding Closed Opens by sliding

Figure 2.3. SEREM Electronics Rogowski coil clamp-on current meters (PAR).

2.3. Hall Effect Sensors

Hall Effect current sensor is based on Hall Effect whose principle is shown in Figure 2.4. In a semiconductor plate (high purity indium arsenide), a voltage (Hall voltage) is induced on two sides of the plate by a magnetic field if a current (Hall current) flows through the other two sides of the plate. The measured hall voltage V_H is proportional to the magnetic field component perpendicular to the plate B and Hall current I_C. The proportionality constant K_H is a property of the sensor material.

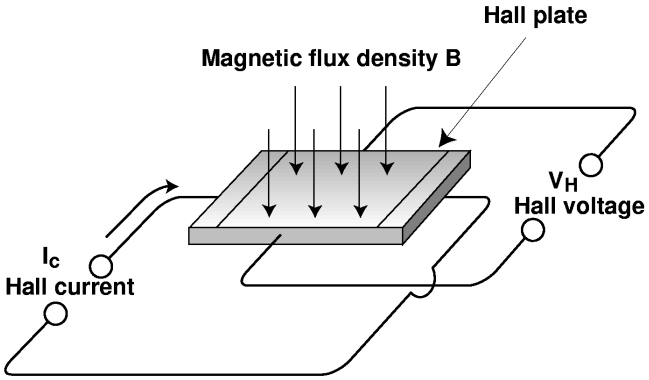

Figure 2.4. Principle of Hall Effect.

A Hall Effect current sensor has several such sensors around the conductor (closed loop sensors, Figure 2.5, left) or on 2 or 3 faces of the conductor (open loop sensors, Figure 2.5, right) or only on one side of the conductor (Figure 3.6). The closed loop sensor in Figure 2.5, left is installed around the 300 kA potline busbars to measure potline current. The open loop sensor in Figure 5, left is used for collector bar current measurements at TRIMET [3]. A commercial version of the

open loop current sensor is shown in Figure 3.1, where it is used for anode current distribution measurements.

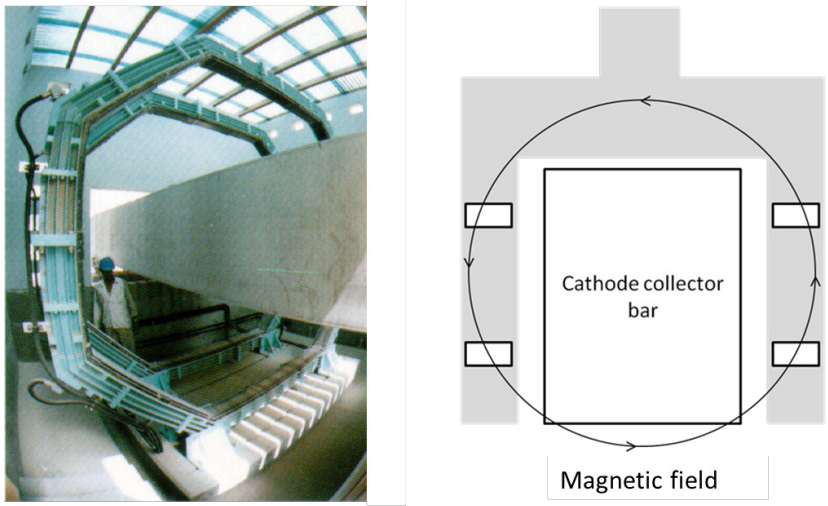

Figure 2.5. Closed loop (left) and open loop Hall current sensor (right [3]).

The electrical current is calculated from Ampere's law, which says that the closed loop integral of magnetic field around a conductor is proportional to the current inside the loop, Equation (2.3).

$$\oint \mathbf{B} \bullet \mathbf{ds} = \mu_0 I \tag{2.3}$$

where: **B** Magnetic induction vector, T
ds Differential length of the path around the conductor, m
• Scalar product of two vectors,
μ_0 and I are defined in Equation (2.2).

The accuracy of the closed loop meter can be as high as 0.1 % , which is required for potline current measurements, but only 5 % for an open loop device, because some magnetic field from other sources than the one from the measured current can be included in the signal where there is no Hall sensor.

2.4 Fibre Optic Current Sensors

Fibre optics current sensors use Faraday Effect to measure electrical current. Faraday found that polarized light traveling along a magnetic field, rotates its plane of polarisation by an angle β proportional to the magnetic field B along the path of light (Figure 2.6 and Equation 2.4). In a current sensor the light travels along a closed path in an optical fibre around the conductor. According to Ampere's law, Equation (2.3), the line integral of magnetic field along the closed loop is proportional to the current enclosed in the loop. The phase shift β is therefore directly proportional to the current enclosed inside the loop of the optical fibre (Equation 2.4). The measured signal is also proportional to the number of times the light travels around the conductor before detection. Optics and electronics is used to produce polarised light and detect the angle of rotation or phase shift of polarised light. The measurement instruments display the current in kA.

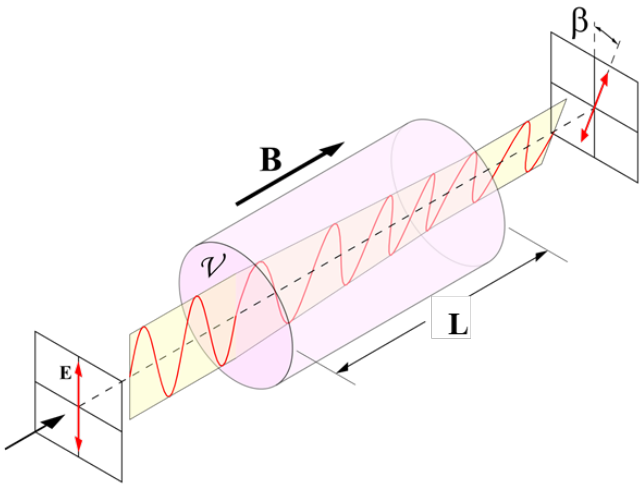

Figure 2.6. Faraday Effect: The plane of linearly polarized light is rotated in the magnetic field parallel to the light travel by an angle β, proportional to the magnetic field (from Wikipedia).

$$\beta = VBL \tag{2.4}$$

For closed loop fibre optics cable:

$$\beta = V\oint \mathbf{B}\bullet\mathbf{ds} = VCNI \tag{2.5}$$

where: β Angle of rotation, radians,
I Electrical current, A,
B Magnetic flux density in the direction of propagation of light, T,
L Length of the path of the light in magnetic field, m,
V Verdet constant, a physical property for the optical fibre material, radians/Tm,
C Constant, depending on specific implementation of the fibre optic sensor,
N Number of turns the light travels around the conductor,
B Magnetic field vector, T,
ds Differential path length vector along the optical fibre in scalar product with vector **B.**

The number of turns the light travels around the conductor increases the strength and the accuracy of the signal detected. Commercial equipment differs in how the polarized light is used and how many turns the optic fibre makes around the conductor. In the examples below all three suppliers, ABB, DynAmp and Smart Digital Optics (SDO) use left and right circularly polarized light. SDO Portable Fibre Optics Current Sensor (SDOP) has the option of one to four loops around the conductor; SDO fixed current sensor also uses multiple loops (Figure 2.7). On the other hand, ABB Fibre Optics Current Sensor (FOCS), Figure 2.8 and DynAmp LKCO use one loop around the conductor with a mirror at the end of the loop, which sends the light back trough the turn and doubles the phase shift ($\Delta\phi_F$ in Figure 2.8) between the left and right circularly polarized light waves, which is the same as having two turns of the fibre around the conductor.

The Verdet constant is temperature dependent, but usually no cooling is required in the fixed systems. However, SDOP is made for hot environment (the cable may rest directly on the busbars) and there is cooling in the flexible cable with a circulating fluid to stabilise the temperature of the optical fibre.

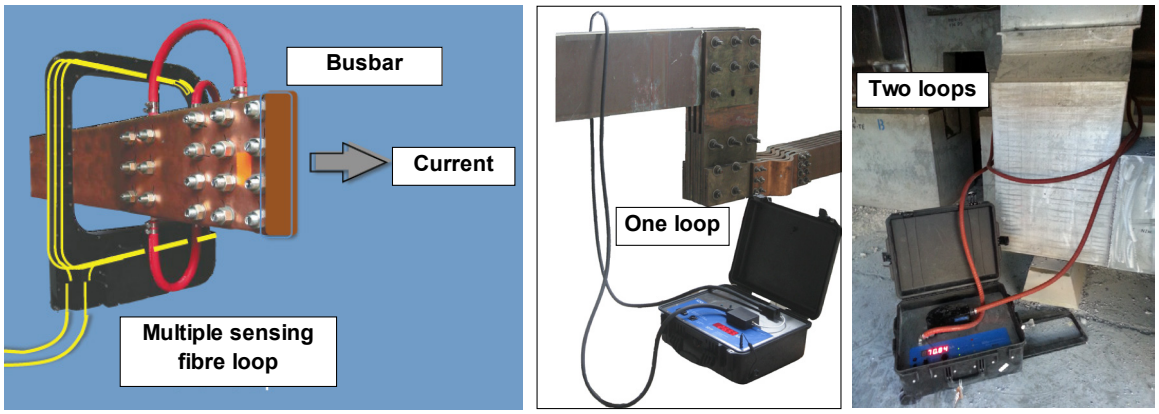

Figure 2.7. SDO Fibre Optics Current Sensors: Left – fixed meter with multiple loops (SDOWCT); Middle – portable sensor (SDOP), used with one loop; Right – portable sensor used with two loops around a busbar.

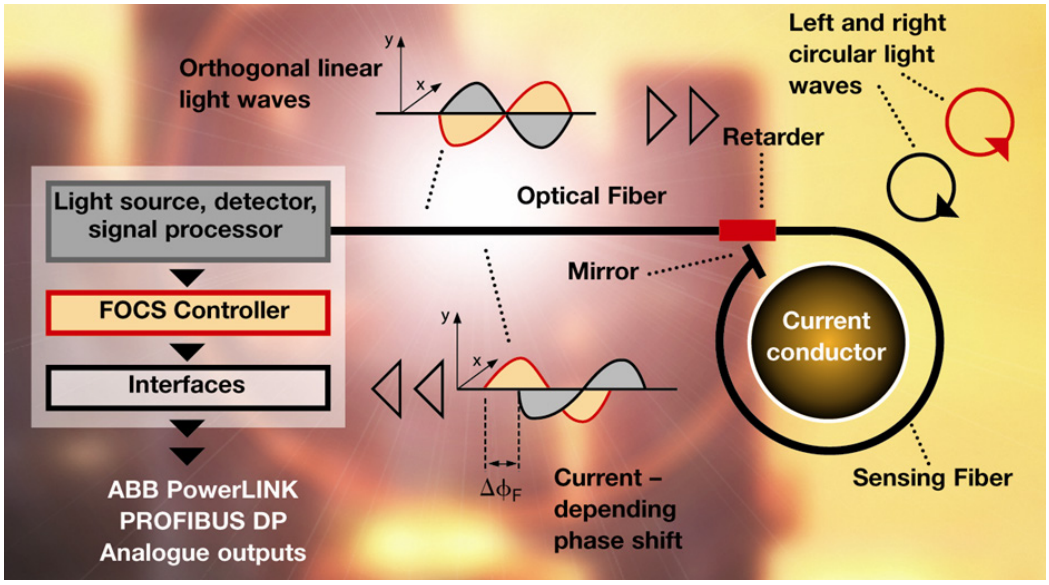

Figure 2.8. Principle of ABB FOCS system using one loop of sensing fibre and a mirror at the end of the loop [9].

Fibre optic current sensors have the following main advantages over the Hall-Effect devices [10]:

- High accuracy of 0.1%, which is maintained over a very wide operating range.
- The design current can be up to 1000 kA.
- The perfect line integration of the magnetic field eliminates erroneous output in case of angled conductor arrangements, inhomogeneous magnetic fields and strong neighbour currents. The magnetic centering of the sensor is not critical.
- Busbar studies are not required to find the optimal placement of the sensor. The sensor installation is straightforward and can be completed in a few hours instead of several days.
- There is no need for onsite calibration.
- Light weight and small size. The Hall sensors used for high-end currents can weigh as much as 2000 kg compared to fibre optic current sensors sensing heads, which weigh less than 15 kg.
- It is easy to install.
- Low maintenance.

In potline current measurements, the fibre optic current sensors have completely replaced Hall-effect instruments in new installations and are gradually replacing the existing Hall-effect devices when maintenance of these is required. Because of their great accuracy of 0.1 %, they are also used as calibration devices for the existing old systems. Two fixed installations are shown in Figure 2.9.

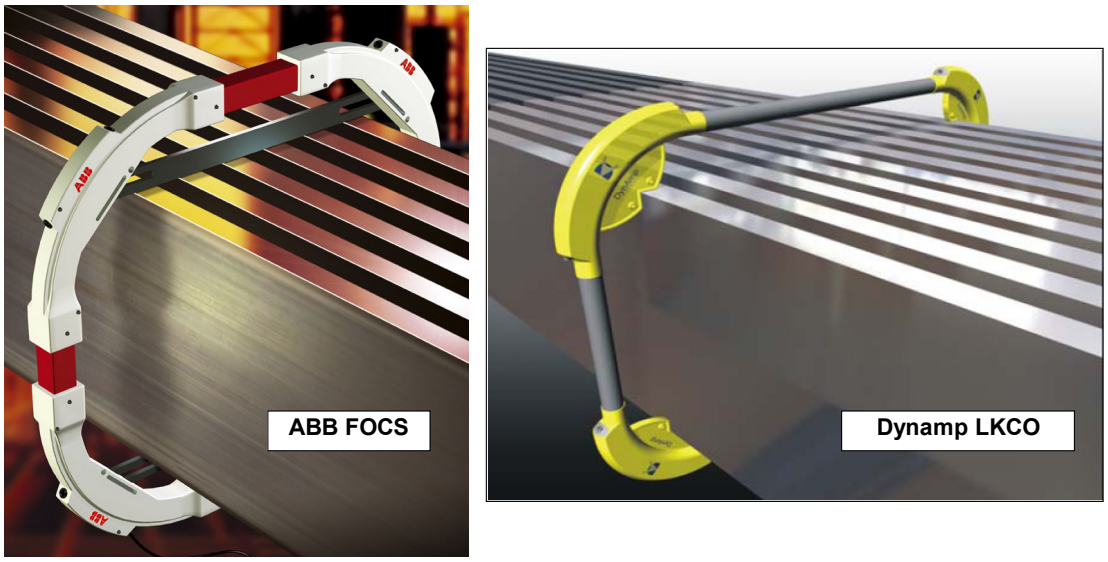

Figure 2.9. ABB FOCS and Dynamp LKCO installations use one loop around busbars with reflecting mirror at the end of the loop.

3. Anode Current Distribution

The anode current distribution in the anodes is most commonly measured in discrete times, which could be once per shift, once per day or only when the pot has problems. For this a portable mV fork is used. It can also be monitored continuously. For this sensors have to be installed permanently on anode rods or on the anode beam. All anodes have to be measured or monitored in order to normalise to pot current.

3.1. Discrete in Time Measurements

3.1.1. Measurement Method and Analysis – Millivolt Fork

The current between the voltage probes on the fork is determined from Ohm's Law, Equation (2.1), applied to anode rod current measurements in Equation (3.2)

With mV fork measurements, anode current distribution is controlled by calculating the average mV of all anodes and then compare individual values to the average. The anodes are moved up or down when the mV are below or above the specified lower and upper limit. If currents in kA are desired, anode current distribution has to be normalized, due to inaccuracies in the measurements, according to Equation (3.1). This formula is derived under the assumption that the anode rod resistivity is equal on each anode. This is not entirely true, because the resistivity depends on temperature which varies from rod to rod. Taking this into account we obtain Equation (3.2). Adding up all the measured anode currents usually does not give the correct line current, because of measurement errors. The anode currents have to be normalized to the true line current with the normalising factor F, Equations (3.3) - (3.4). Combining Equations (3.2) to 3.4, we get Equation (3.5). It appears immediately that the resistivity is a correction factor and

that we obtain Equation (3.1) from Equation (3.5) if the rod temperatures are assumed to be equal.

$$I_i = \frac{\Delta V_i}{\sum_1^N \Delta V_i} I \qquad (3.1)$$

$$I_i = \frac{\Delta V_i A}{\rho(T_i) L} \qquad (3.2)$$

$$F = \frac{I}{\sum_1^N I_i} \qquad (3.3)$$

$$I_{inorm} = I_i F \qquad (3.4)$$

$$I_{inorm} = \frac{V_i}{\rho(T_i)} \frac{I}{\sum_1^N \frac{V_i}{\rho(T_i)}} \qquad (3.5)$$

where: I_i Individual current in anode i, kA
I Measured potline current, kA
I_{inorm} Normalized individual anode current, kA
ΔV_i Measured voltage drop in anode i, mV
N Number of anodes
A Anode rod cross-section, m^2
L Distance between the tines of the mV fork, m
$\rho(T_i)$ Electrical resistivity of anode rods i, μΩm.
T_i Temperature anode rod I between the two tines of the fork, °C

In normal potroom measurements with mV fork, the anode rod temperature is not measured. This induces and error in measurements because electrical resistivity is temperature dependent. In a special measurement campaign on DX+ pots it was determined that the anode rod temperatures at any given time vary by approximately 50 °C or ± 25 °C from the average. Ignoring this temperature variation induces an error of ± 7 % in anode current. Another error of ± 3 % is induced by reading the mV only to one figure behind the decimal point. The combined maximum error of mV is fork is ± 10 %. The combined probable error, which is calculated as the square root of the squares of individual errors, is ± 8 %. This is good enough for anode current control which typically does not have upper and lower control band for adjustments of less than ± 20 %.

3.1.2. Comparison of Three Methods for Anode Current Distribution

Figures 3.1 and 3.2 show the comparison of three methods for anode current distribution measurements: SDOP, mV fork and VHE current meter. If the anode currents are measured directly in kA, they are normalized according to Equations (3.3) and (3.4). The normalization factor F for SDOP is 0.998 (the deviation from potline current is – 0.2 %) and for VHE current meter it is 1.041 (the deviation from potline current is 4.1 %). The normalized mV fork currents are determined directly from Equation (3.1) because the anode rod temperature was not measured. The normalization factors include the precision of the instruments and the variation of anode currents during the time of measurement. The SDOP is very accurate and will be taken as calibration instrument.

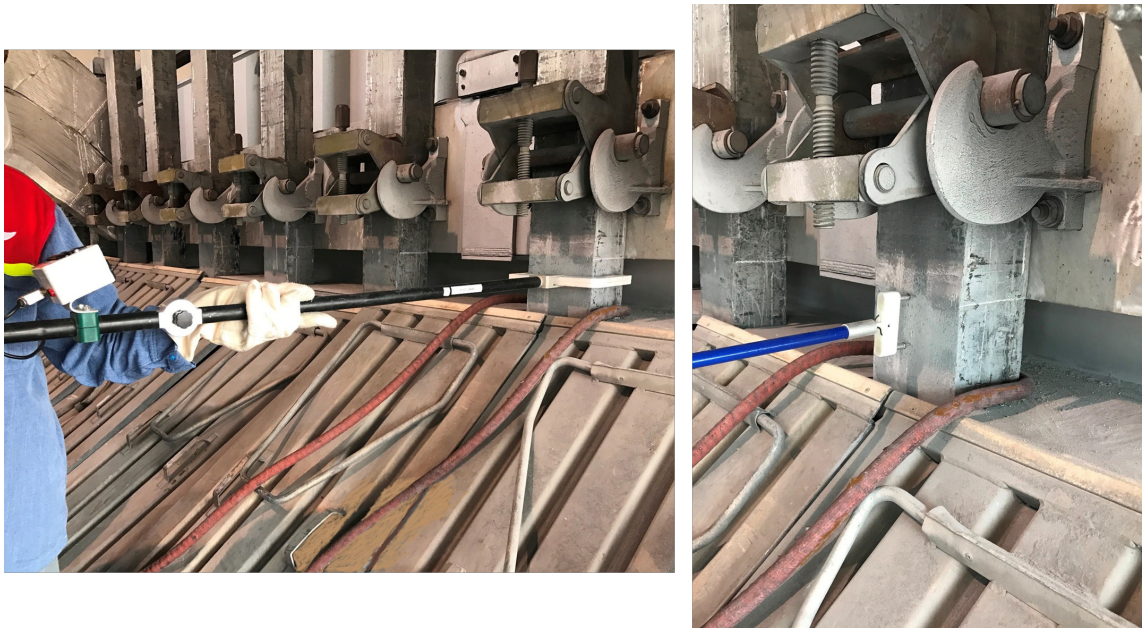

Figure 3.1. Anode current distribution measurement. Left – with SDOP (the hose around the rod) and VHE Anode Current Metre; Right – with mV fork and SDOP.

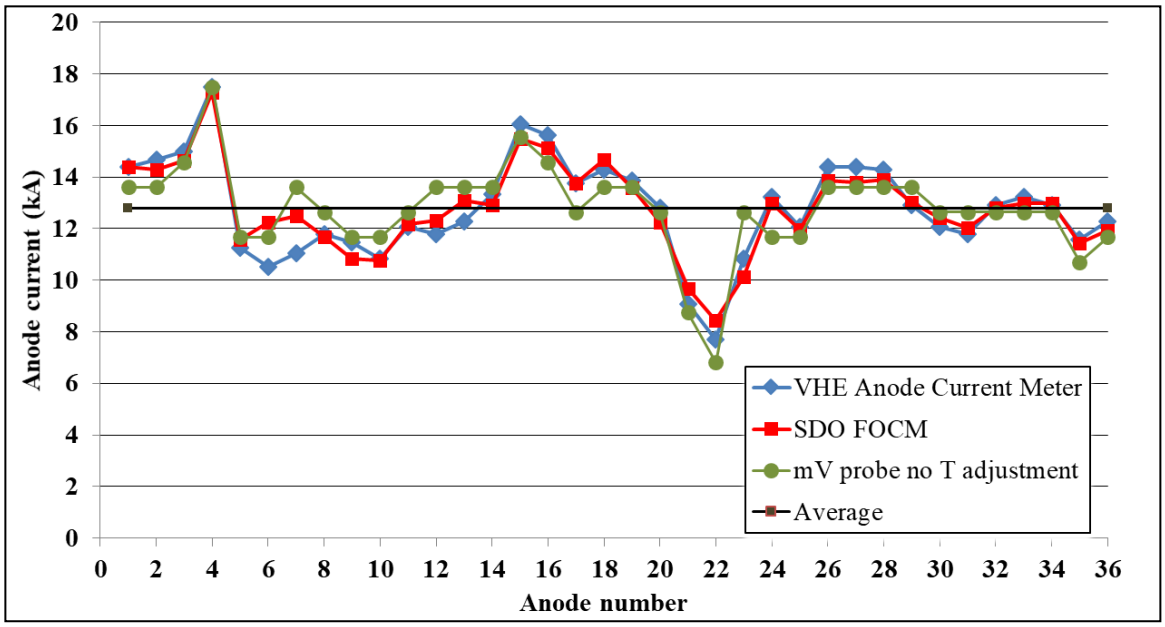

Figure 3.2. Anode current distribution measured with three methods, indicated in the legend and shown in Figure 3.1. The curve for mV fork is with no temperature adjustment as in normal pot operation practice. Anode No 4 was 5 days old and was flagged to be raised. Anodes 21 and 22 were less than 1 day old.

We can see that the mV and VHE methods generally follow the SDO measurements, with average absolute and individual maximum deviations are: 3.4 % average and + 7, -14 % maximum for VHE and 5.4 % average and + 14, - 25 % for mV fork.

3.2. Continuous Measurement of Anode Currents

3.2.1. Using Voltage Drop (mV) Measurements

Figures 3.3 and 3.4 show three methods of continuous anode current distribution measurement. The calculation of current between the probes according to Equation 3.2 assumes uniform current distribution in the busbar cross-section. This is certainly true for anode rod forks (Figure 3.3 left). Accuracy of the measurement will suffer if this is not the case, which could happen on the anode beam (Figure 3.3 right and Figure 3.4) because the anode beam cross section is large and the distance between anode probes is quite small. This should be checked with modelling and adjusted if required.

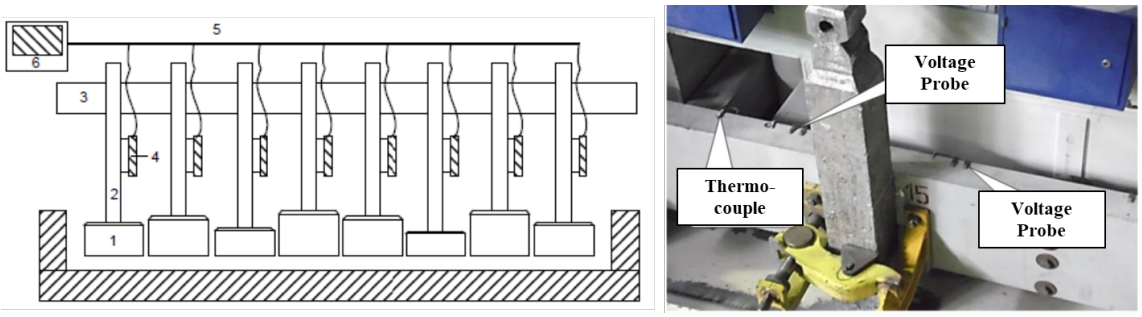

Figure 3.3. Continuous measurement of individual anode currents with mV forks [6] (left) and with voltage probes on the anode beam [11] (right). 1- anode, 2- anode rod, 3- anode busbar, 4 – mV fork, 5 - data line, 6 - data controller.

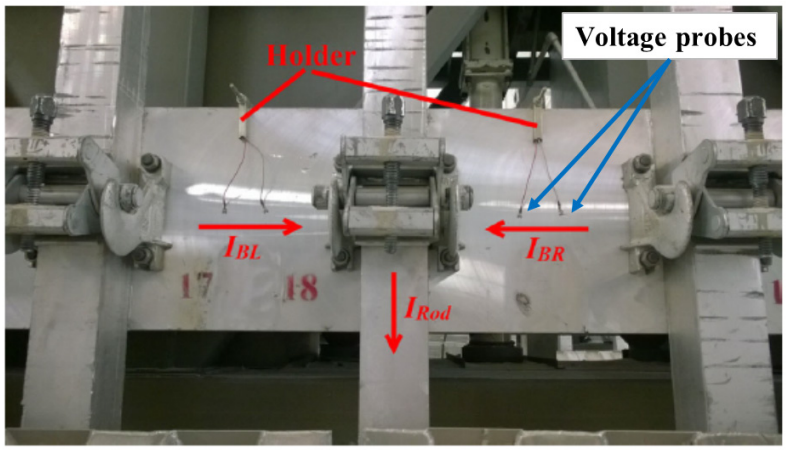

Figure 3.4. Measurement of individual anode currents with voltage probes on the anode beam. $I_{Rod} = I_{BL} - I_{BR}$ [15].

Continuous individual anode current monitoring has been demonstrated to have the following additional benefits over the discrete anode current measurements:

1) Early prediction of anode effects (current decreases in anodes with low concentration of alumina because of increased bubble coverage). [11, 12, 14]
2) Prediction of crust-breaker problems where alumina does not enter the bath (lower local concentration of alumina decreases currents in adjacent anodes) [11, 12].
3) Prediction of anode spikes (anode with spikes carries larger current and is very noisy) [8, 11]. Figure 3.5 shows the detection of spikes on an anode.
4) Analysis of MHD instabilities and identifying the anodes that may be the cause [6].
5) Helps understanding background PFC emissions [7]

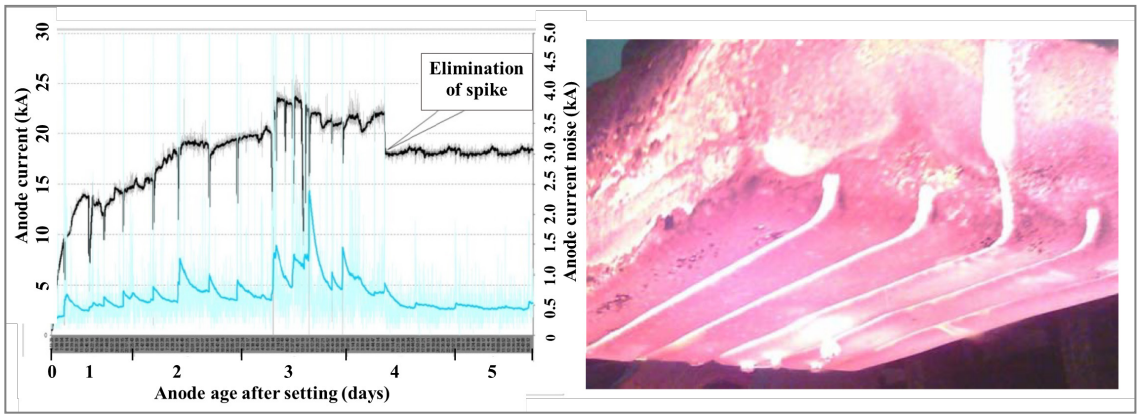

Figure 3.5. Left: Dynamics of anode current (black curve) and anode current noise (blue curve) during 5 days after poor quality anode setting [11]. Right: The same anode with spikes on day 4. Average anode current is approximately 17.7 kA.

3.2.1. Using Hall Sensors

The first application of Hall sensors for continuous anode rod current monitoring, by measuring the magnetic field generated by the anode rod current, was reported in [5], but it was not commercialized because it was too costly.

More recently, the Wireless Industrial Technologies (WIT) developed a system which determines the anode rod currents by measuring the magnetic field generated by the current flowing in the anode rod. Two Hall Effect sensors are incorporated in a circuit, called a "slave" placed next to and behind each anode rod, fixed on the bottom of anode busbar. The slaves are wired along a single cable to one of two "masters" that are placed at the end of the pot. The cable serves to both bring power to the slaves and as a route for data to flow to the masters, which then relay the data wirelessly to a receiving computer ("manager"). The system and industrial testing are is described in references [12 - 14]. Figure 3.6 shows two installations of the WIT and Figure 3.7 gives a comparison between the mV measurements on anode rods and WIT as shown in Figure 3.6 right.

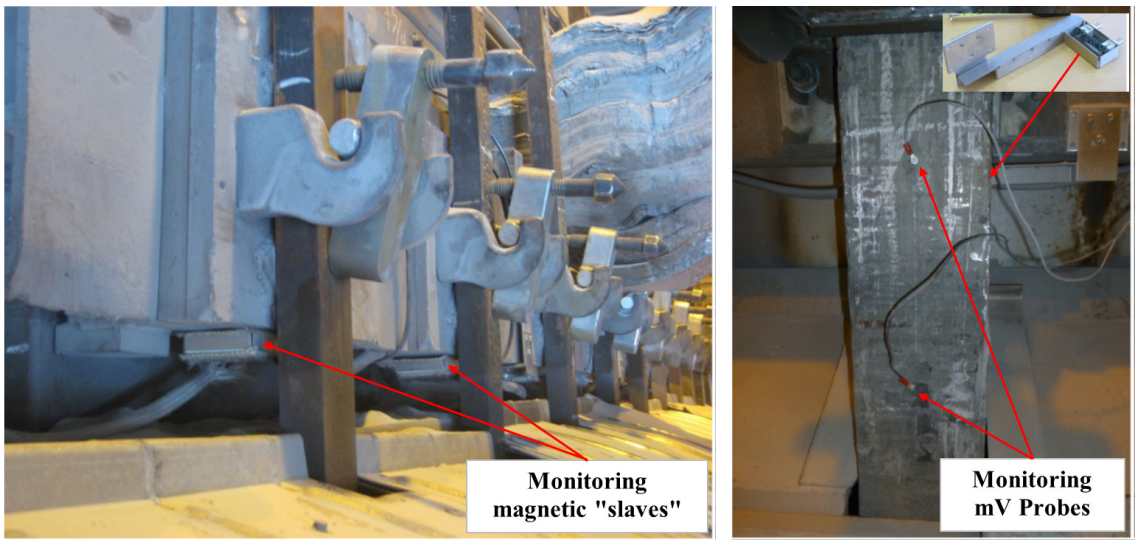

Figure 3.6. Left: Monitoring magnetic slaves on a test pot in Wenatchee Smelter, USA [12]. Right: TRIMET pot - magnetic slave is behind anode rod and shown outside in right top corner compared to continuous monitoring mV probes [13].

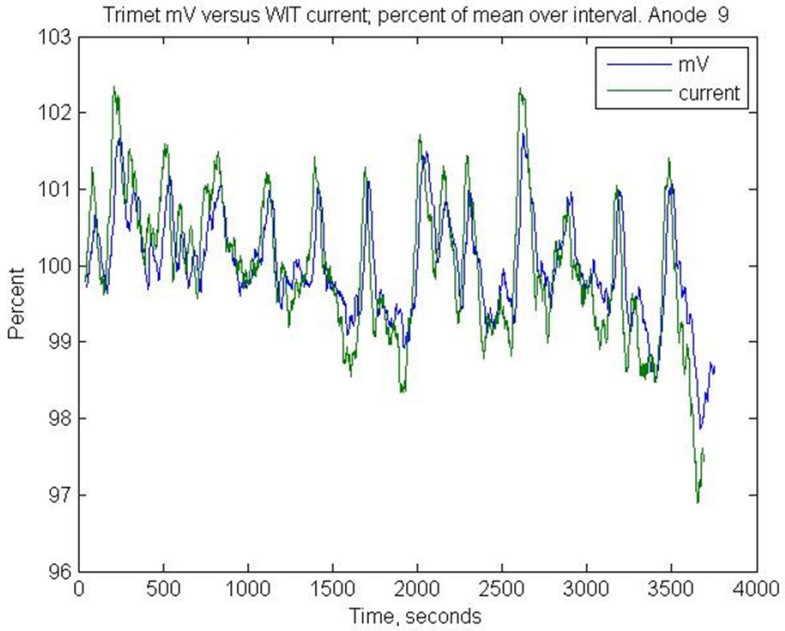

Figure 3.7. Comparison of WIT magnetic slave and mV probe signals on a TRIMET experimental pot [13].

4. Measurement of Cathode Collector Bar Currents

The measurement of cathode collector bar current distribution is more difficult than in anode rods for several reasons:

- There is no solid straight conductor between each collector bar and the cathode busbar. Instead there is a flexible made of thin leaves in which the current is not uniformly distributed as some leaves are longer than the others.
- The voltage drop can only be measured across the full length of the flexible.
- If the voltage drop method is chosen, the temperature is difficult to measure because it cannot be taken on the flexible. Often there is also plenty of dust and debris on the top.
- Clamp-on or open jaw Rogowski coil cannot be used because there is not enough room to open the loop.
- Open loop Hall sensor devices also have too limited access, but these are nevertheless used in some companies [3].
- For safety, the measurement should be made from the potroom floor even if the potroom has a basement. This is particularly important if the purpose of the measurement is to determine on high iron pots if a collector bar has been attacked. However the usual floor grill between the two pots often does not have enough room to pass any instrument through, except individual voltage probes.

Below, we compare the voltage drop method with SDOP, portable fibre optics current meter. The purpose of the measurements was to validate the mathematical model of the busbar design and to check if the voltage drop method is accurate enough to detect cathode collector bar or cathode block problems.

The voltage drop method is illustrated in Figure 4.1, applied to the new EGA cathode flexible design. The measurement was part of the contact voltage drop control. Only the voltage drop between points A and B was used for current distribution measurements; the bolted contact voltage drop (B - C) must be excluded from the calculation because it may not be proportional

to the current if the contact is poor. The temperature of the flexibles was not measured, because it would be too time consuming to do it; this means that the same temperature was assumed for each collector bat. The normalization was carried out as per Equations shown in Equations (3.1) to (3.4).

The voltage drop method was compared with the precise SDOP measurement. The optical fibre hose was wrapped around each cathode flexible once. All 56 collector bars were measured. The results were normalized to potline current as per Equations (3.3) to (3.4). The normalization factor for SDOP measurement was 1.0028, which means that the total sum of currents of all collector bars was only 0.28 % lower than the potline current, measured at the rectifier output. The SDOP measurements can be considered as very precise calibrator. The comparison of the two methods is shown in Figure 4.2.

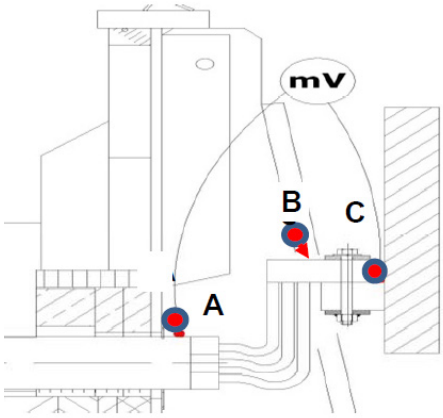

Figure 4.1. Cathode flexible voltage drop A-B is used to calculate cathode collector bar current distribution [16].

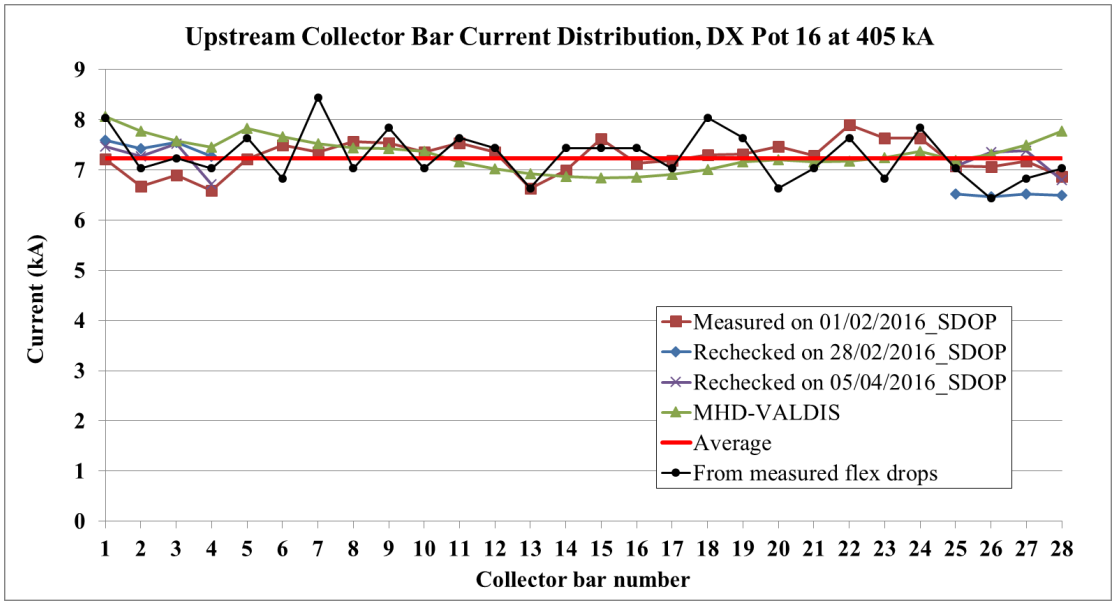

Figure 4.2. Collector bar current distribution measured with cathode flexible mV method and SDOP, compared to MHD-VALDIS model design calculations.

The currents in the four upstream collector bars at each end were repeated twice more, one and two months later. The results show some sensitivity of collector bar currents to pot condition. For example, on 28/02/2016, the four collector bars at tap end (No. 25 to 28) carried less current

than one month before. The reason was that the measurement was done only 6 h after the change of the two corner anodes above these collector bars. The conclusion was that the cathode surface below these changed anodes had some freeze because of the anode change, which prevented some current to enter into the cathode blocks.

The currents calculated from the cathode flexible voltage drop measurements agree fairly well with SDO measurements; therefore, the former can be used as indication of collector bar current distribution. The measurement also confirmed that the upstream / downstream current balance was within ± 1 % as predicted by the busbar design model.

5. Measurement of Busbar Currents

Three DX+ pots were instrumented with voltage probes and thermocouples between the probes on all the cathode busbars, 6 upstream and 6 downstream that constitute the full pot current when added up. The probes were 1.5 to 2.4 m apart. The busbar temperatures and currents were continuously monitored for several years, with very few failed voltage probes and thermocouples; these were replaced if they broke down. For the analysis, the data had to be filtered, because some spurious values were recorded from time to time. A simple filter was devised, which replaced a spurious value with average value of the last 10 readings. The normalization factor of the total measured average currents over a period of 3 to 4 weeks in December was 1.037, 1.60 and 1.077 in the three cells. The measured currents from mV drop were lower than the current measured at the rectifiers. Busbar temperatures were from 13 to 21 °C (average of 17 °C) hotter in July than in December at 440 kA.

On 28 October 2013, DX+ Eagle currents were also measured with SDOP. The normalization factor for these was from 1.002 to 1.010, i.e., the difference with the potline current was 0.2 to 1.0 %. This does not define the accuracy of SDOP, but rather shows that the precise busbar current distribution may have shifted somewhat during the measurement time. Indeed after five hours of measurement, the first busbar was re-measured and the result was somewhat different than five hours earlier. In the meanwhile, the wind changed direction.

6. Conclusions

Several measurement techniques for busbar, anode rod and cathode collector bar current distribution are available. For main potline current measurement, fibre optics current sensors are the exclusive devices to use in new installations and are replacing the previous Hall sensors whenever major maintenance of these is required. The potline current meters have an accuracy of 0.1 % and are a standard for normalisation of currents obtained by any other method on each individual pot. The portable SDO fibre optics current sensor (SDOP) is also a very accurate instrument and can be used as a calibration unit for any other instrument.

A considerable amount of research and development has gone into anode current distribution measurements, particularly continuous, in order to control the currents within the specified limits or to find and predict process deviations, such as anode spikes and anode effects. The simplest and most economical method is the measurement of voltage drop in the conductor over a fixed distance. It is hard to assure the accuracy of any economical method better than ± 10 % in all circumstances. It is not sure that any of the available methods will be cost effective and practical enough to balance the cost to benefit on a full potline in a foreseeable future.

7. References

1. Jean-Paul R. Huni, Individual anode control, *Light Metals* 1987, 199-202.
2. Abdalla Zarouni et al., Mathematical model validation of aluminium cells at DUBAL, *Light Metals* 2013, 597-602.
3. Matthias Dechent and Richard Meier, Implementation of a new measuring device for cathode current distribution, *Proceedings of 35th International ICSOBA Conference*, *Travaux No.* 46, Hamburg, Germany, 2 – 5 October 2017, Paper AL32.
4. Benoit Verreault, Réjean Fournier, Christian Bourbonnière, Millivolt Anodes and Cicero - new tools for better pot and potline control, *Proceedings of 33rd International ICSOBA Conference*, *Travaux No. 44,* Dubai, UAE, 29 November – 1 December 2015, Paper AL11, 589-597.
5. Jim Barclay, Oliver Hung, Joe Rieg, Control electrochemical cell dynamics with electrode current measurement, *Light Metals* 2001, 1219-1224.
6. Jeffrey Keniry and Eugene Shaidulin, Anode signal analysis - the next generation in reduction cell control, *Light Metals* 2008, 287-292.
7. Ali Jassim et al., Studies on background PFC and current distribution using individual anode signals in aluminium reduction cells, *Proceedings of 33rd International ICSOBA Conference*, *Travaux No. 44,* Dubai, UAE, 29 November – 1 December 2015, Paper AL25, 737-749.
8. Ali Jassim et al., Studies toward balancing the current in smelting cells, *Proceedings of 11th Australasian Aluminium Smelting Technology Conference*, Dubai, 6 – 11 December 2014, Paper 09M6.
9. Erik Haitjema, Upgrading outdated rectifier control systems with an AC 800PEC digital controller, Presentation at TMS 2006 Annual Meeting, March 12 – 16, 2006, San Antonio, USA.
10. M. Wiestner, M Wendler, K. Bohnert, Technology leap in DC current measurements opens new opportunities for aluminium smelters, Retrieved from http://new.abb.com/power-electronics/focs, Article, Reprint from Aluminium 2005, 1-2.
11. Iliya I. Puzanov et al., Continuous monitoring of information on anode current distribution as means of improving the process of controlling and forecasting process disturbances, *Journal of Siberian Federal University, Engineering & Technologies*, 2016, 9(6), 788-801 (in Russian).
12. James W. Evans and Nobuo Urata, Wireless and non-contacting measurement of individual anode currents in Hall-Héroult pots; experience and benefits, *Light Metals* 2012, 939-942.
13. Andreas Luetzerath, On-line monitoring of individual anode currents at TRIMET Aluminium, Hamburg, Germany, *Proceedings of 32nd International ICSOBA Conference*, *Travaux No. 43,* Zhenzhou, China, 29 November – 1 December 2014, Paper AL03.
14. Lukas Dion et al., On-line monitoring of individual anode currents to understand and improve the process control at Alouette, *Light Metals* 2015, 723-728.
15. Hongliang Zhang et al., Progress in aluminum electrolysis control and future direction for smart aluminum electrolysis plant, JOM, Vol. 69 No. 2, 2017, 292-300.
16. Lalit Kumar Mishra et al., New connections for cathode flexibles in aluminium electrolysis cells, *Proceedings of 35th International ICSOBA Conference*, *Travaux No.* 46, Hamburg, Germany, 2 – 5 October 2017, Paper AL31.